

Synthetic α -Helix Mimetics as Agonists and Antagonists of Islet Amyloid Polypeptide Aggregation**

Ishu Saraogi, James A. Hebda, Jorge Becerril, Lara A. Estroff, Andrew D. Miranker,* and Andrew D. Hamilton*

The development of small molecules that can modulate the damaging effects of protein aggregation processes remains a high priority goal in contemporary medicinal chemistry.^[1] An important class of these aggregates, called amyloids, has been implicated in numerous degenerative diseases including Alzheimer's, type II diabetes, senile systemic amyloidosis (SSA), prion diseases, and rheumatoid arthritis. The attribute shared by these symptomatically unrelated diseases is that a normally soluble protein undergoes a conformational change resulting in self-assembly into cytotoxic forms, culminating in a β -sheet-rich fibrillar structure. Islet amyloid polypeptide (IAPP), or amylin, is one such protein which has been implicated in amyloidogenesis in type II diabetes.^[2] IAPP is cosecreted with insulin by the β cells of the islets of Langerhans and an aggregated form of IAPP is believed to play a role in β -cell toxicity in the pathology of type II diabetes.^[3]

Amyloid-forming processes proceed by a nucleation dependent reaction mechanism. The structural and energetic basis for nucleation is, however, poorly understood.^[5] For IAPP, Knight and Miranker^[6] proposed a possible mechanism where nucleation is initiated by the binding of IAPP to cell membranes through contacts mediated by residues 1–20 (Figure 1 a).^[4] The region of IAPP comprising residues 5–19 clearly shows a helical structure having positive charges predominant on one face, and likely forms multihelical aggregates upon interaction with the membrane surface.^[7,8] The formation of these α -helical intermediates accelerates the assembly of the amyloid structure which is rich in β sheets.^[9]

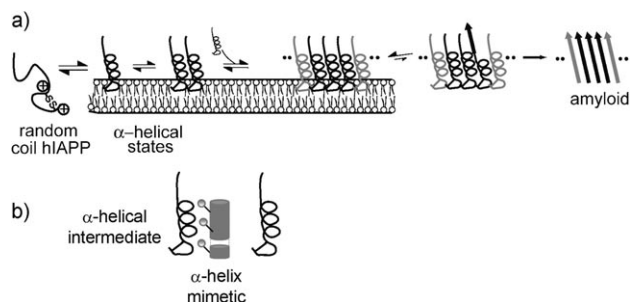


Figure 1. a) Model for IAPP amyloid formation with α -helical intermediate states.^[4] b) Schematic representation of an α -helix mimetic of varying length, interacting with the α -helical intermediate in the IAPP fibril formation pathway.

Recent findings have additionally suggested that these helical oligomeric intermediates may be the relevant cytotoxic form of IAPP.^[8,10] An interesting, and previously unexplored, potential therapeutic approach for mitigating the cytotoxic effects of IAPP would be to design molecules that interfere with the helix assembly process (Figure 1 b).

Inhibition of IAPP aggregation by small molecules based on a rhodanine scaffold,^[11] phenol red,^[12] and phenolsulfonphthalein^[13] has been reported. Similar disruption of amyloid assembly in other protein aggregation diseases by aromatic dyes is known.^[14,15] A plausible general mechanism for such inhibition involves π stacking of the dye with the aromatic amino-acid-rich core of the developing amyloid.^[12,15] In this work, we propose an alternative mechanism of amyloid inhibition wherein we target the transient α -helical intermediates in IAPP aggregation.

We have previously reported synthetic structures that mimic the residues along one face of an α helix and successfully disrupt important protein–protein interactions.^[16] In particular, the oligopyridylamide scaffold **1** uses intramolecular hydrogen bonding to rigidify the backbone, and projects functionality on one face of the molecule in direct analogy to an α helix.^[17–19]

An inspection of the N-terminal region of human IAPP (hIAPP) reveals four positive charges in close spatial proximity: Arg11 and His18 (which is likely protonated at the membrane surface) in the helical domain, as well as Lys1 and the N-terminus. A potential size and charge complementarity with this region might be achieved by a tetrameric or pentameric form of the oligopyridylamide scaffold containing four or five carboxy-terminated side chains, respectively. To study systematically the effect of an increasing number of negative charges on interaction with IAPP, the monomeric

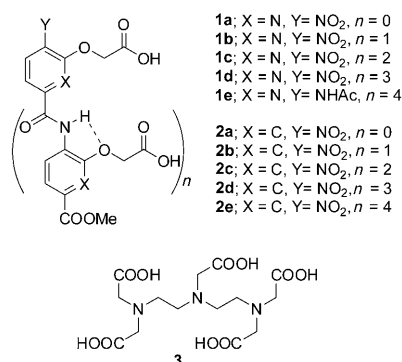
[*] J. A. Hebda,^[1] Prof. A. D. Miranker
Molecular Biophysics and Biochemistry, Yale University
266 Whitney Avenue, P.O. Box 208114
New Haven, CT 06520-8114 (USA)
Fax: (+1) 203-432-3104
E-mail: andrew.miranker@yale.edu

I. Saraogi,^[1] J. Becerril, L. A. Estroff, Prof. A. D. Hamilton
Department of Chemistry, Yale University
225 Prospect Street, P.O. Box 208107
New Haven, CT 06520-8107 (USA)
Fax: (+1) 203-432-6144
E-mail: andrew.hamilton@yale.edu

[†] These authors contributed equally to the work.

[**] We thank Prof. G. W. Brudvig for suggestions and Dr. C. Incarvito for assistance with X-ray crystallographic analysis. This work was supported by National Institutes of Health grants to A.D.H. (GM69850) and A.D.M. (NIDDK DK079829). J.A.H. was supported by a NRSA fellowship (AG031612).

Supporting information for this article is available on the WWW under <http://dx.doi.org/10.1002/anie.200901694>.



through pentameric pyridylamides **1a–1e** were synthesized. Furthermore, to probe the efficacy of the hydrogen-bonding preorganization effect in these molecules, the corresponding oligobenzamide series **2a–2e** was synthesized,^[18,20,21] in which the pyridine rings were replaced by benzene so that bifurcated hydrogen bonding was no longer possible. These molecules have greater conformational flexibility about the aryl-C(=O) bonds and permit an adaptability of structure on binding, albeit at an entropic cost.

The molecules were synthesized using linear solution-phase iterative coupling as reported earlier for the shorter homologues.^[18,19] Briefly, chain elongation was achieved using successive amide coupling and nitro group reduction steps (see the Supporting Information). The acid groups, which were protected as *tert*-butyl esters, were cleaved in the last step to give the target compounds.

The dimers (**1b**, **2b**) and trimers (**1c**, **2c**) have previously been shown to adopt an elongated rod-like conformation in the solid state with a more curved backbone in the oligopyridylamides than the oligobenzamides.^[18] This effect continues in tetrameric **1d** and pentameric **1e**, as seen from their crystal structures (Figure 2), and the side chains project from one face of the molecule, forming a recognition surface for potential binding to a complementary face of an α helix. As a result of some positional disorder, only four of the five side chains in the crystal structure of **1e** could be modeled. However, the location of the oxygen atom of the side chains, as identified from the electron density map, allows us to conclude that **1e**, like its shorter homologues, adopts an extended curved conformation with the side chains projected on one face. Molecular modeling studies with **2d** and **2e** suggest that they adopt a similar extended conformation, with less certainty over the position of the side chains.^[20]

IAPP binds lipid membranes and its fibrillization is strongly accelerated in the presence of liposomes containing mixtures of anionic dioleoylphosphatidylglycerol (DOPG) and zwitterionic dioleoylphosphatidylcholine (DOPC).^[6] The kinetic profile is characterized by a lag phase with a subsequent cooperative transition into the aggregated state. The rate of fibrillogenesis of IAPP under lipid-catalyzed conditions, in the presence of the helix mimetics, was determined using an exogenous fluorescent dye, thioflavin-T (ThT). ThT binds specifically to amyloid fibrils without significantly disturbing the IAPP fiber formation pathway,^[6] and the relative fluorescence intensity is an indicator of the

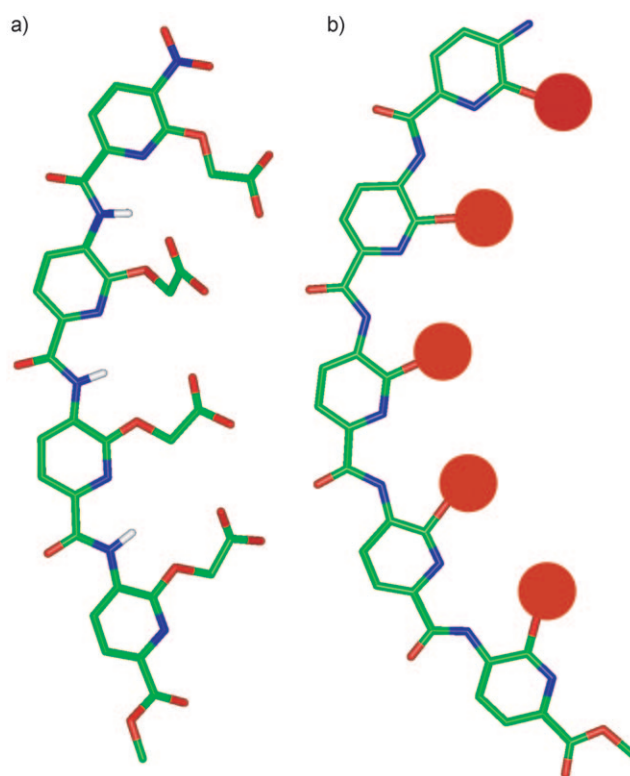


Figure 2. a) X-ray crystal structure of the *tert*-butylester of **1d** (*t*Bu ester groups and non-NH hydrogen atoms have been omitted for clarity). b) Crystal structure of the backbone of **1e** (Y = NH₂), the side chains could not be modeled because of positional disorder, and are shown as red balls. Red O, blue N, green C, white H.

transition into the amyloid state. Since compounds that interact with IAPP and affect fiber formation can interfere with ThT binding, our analysis of changes in amyloid formation kinetics was limited to the midpoint of the transition, t_{50} , rather than the absolute ThT signal.

In the presence of the helix mimetics, the rate of acceleration of lipid-catalyzed IAPP fiber formation was significantly diminished. A representative kinetic data plot for **1e** is shown in Figure 3a. Molecule **1e** was an effective inhibitor of the lipid-catalyzed IAPP fiber formation with a relative t_{50} that is four-fold higher than the control reaction. This inhibition was dose-dependent and an IC₅₀ of 8 μ M was obtained (Figure 4a) under the conditions of the assay. Electron microscopy images obtained after one hour in the presence of **1e** under lipid-catalyzed conditions confirmed the much slower growth rate of fibers (Figure 4b,c). NMR-binding experiments with rat IAPP, which does not form fibers, showed a discrete binding interaction between **1e** and IAPP with an approximate K_d value of about 40 μ M (see the Supporting Information).

For both series of compounds, a comparison of the relative t_{50} values for the lipid-catalyzed aggregation showed a gradual increase in antagonistic activity from the dimer to the longer oligomers, whereas the monomer had virtually no effect on the kinetics (Figure 5a). The activities of the tetramers and the pentamers were comparable although the pentamers were slightly less active in both cases.

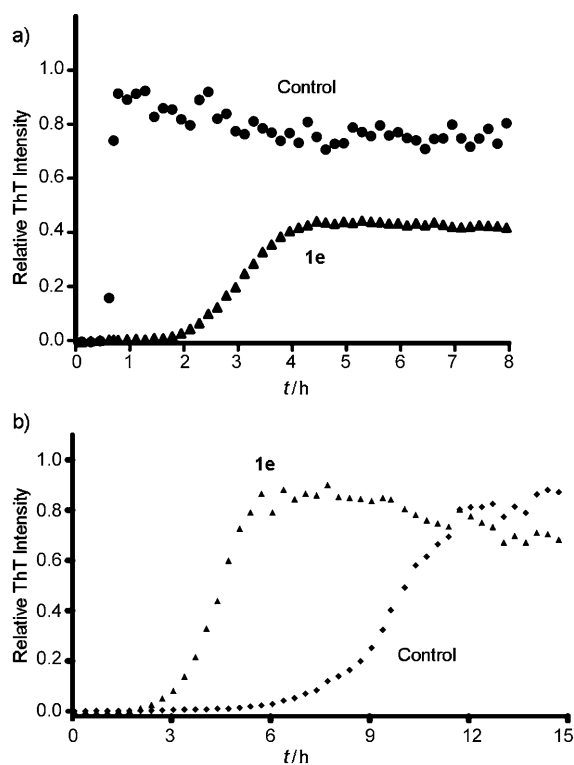


Figure 3. Relative rate of hIAPP ($10\ \mu\text{M}$) aggregation in the presence of **1e** ($100\ \mu\text{M}$) compared to the control reaction showing: a) inhibition under lipid-catalyzed and b) acceleration under lipid-free conditions.

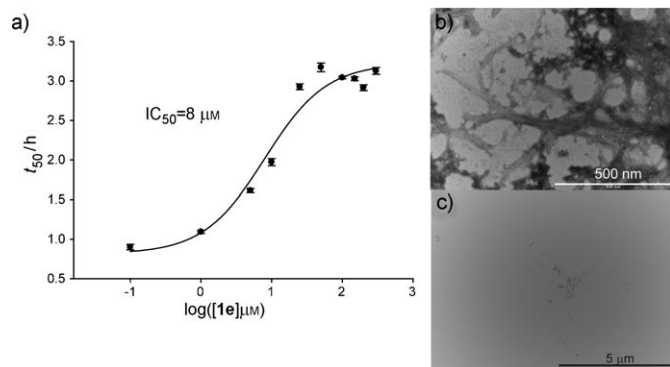


Figure 4. a) Dose response curve for lipid-catalyzed IAPP amyloid inhibition with **1e**. Electron microscopy pictures showing: b) the presence of fiber formation in the control reaction and c) absence of fiber formation with **1e** under lipid-catalyzed conditions after 1 h.

To probe the mechanism of inhibition of aggregation, kinetic experiments were performed in the absence of the lipid. Under these conditions, the molecules acted as agonists of amyloid formation and compound **1e** showed two- to three-fold acceleration in the aggregation kinetics (Figure 3b). As with the lipid-catalyzed conditions, the rate of acceleration was proportional to the length and charge of the compounds, and the pentamers in both the series were the most effective accelerants (Figure 5b). However, under lipid-catalyzed conditions, higher bulk concentrations of the compounds were required to strongly affect fiber formation (Figure 5a versus Figure 5b) presumably because under these

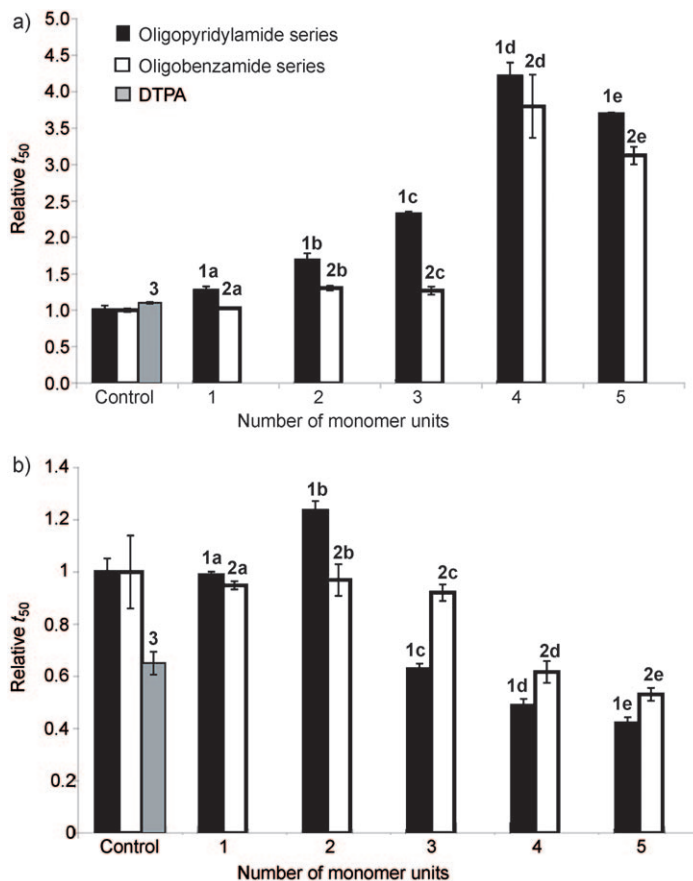


Figure 5. Bar charts showing comparison of the relative rates of fiber formation with the designed molecules; [hIAPP] = $10\ \mu\text{M}$. a) Inhibition under lipid-catalyzed conditions: DOPG/DOPC = 1:1 ($500\ \mu\text{g mL}^{-1}$); [compound] = $150\ \mu\text{M}$, and b) acceleration under lipid-free conditions: [compound] = $10\ \mu\text{M}$.

conditions the compounds do not effectively partition into the membrane while IAPP is bound at the membrane surface.

Diethylene triamine pentaacetic acid (DTPA; **3**), a control molecule bearing five carboxylic acid groups in a less well-defined orientation, had very little effect on the kinetics of aggregation (Figure 5). Whereas the lipid-catalyzed kinetic data were virtually indistinguishable from the control, DTPA accelerated the de novo fiber-formation kinetics somewhat, perhaps as a result of nonspecific charge neutralization effects. Control molecules bearing positively charged (based on **1c**^[22]) or *tert*-butyl ester protected (**1c_{ester}** and **1e_{ester}**; see the Supporting Information for structures) side chains also had little effect on lipid-catalyzed kinetics of aggregation (see the Supporting Information). The lipid-free kinetics for **1c_{ester}** and **1e_{ester}**, however, were not directly comparable to **1e** presumably because of their hydrophobicity and highly aggregating nature. Taken together these data suggest that the number, nature, and orientation of the charges are crucial to the activity of the molecules, indicating a specific interaction most likely with the complementary α -helical region of IAPP. A detailed mechanistic study will be reported elsewhere.^[23]

In conclusion, two series of compounds based on an oligoamide backbone were designed to provide a comple-

mentary surface to interact with the α -helical domain on IAPP. These molecules project their anionic substituents at the right distance and orientation, and under lipid-free conditions accelerate the aggregation of IAPP. Under lipid-catalyzed conditions, however, they retard the formation of amyloid deposits. Whereas both series of compounds follow the same general trend, the oligopyridylamide series shows a slight, but consistently higher effect potentially resulting from a reduced entropic penalty upon binding (see the Supporting Information). This study suggests the targeting of discrete amyloidogenic intermediates as an alternative therapeutic approach to amyloid diseases and paves the way for research into novel type II diabetes drugs having a particular focus upon inhibiting the lipid-catalyzed acceleration of IAPP aggregation.

Received: March 28, 2009

Revised: October 13, 2009

Published online: December 22, 2009

Keywords: α -helix mimetics · amyloid β -peptides · diabetes · helical structures · proteomimetics

- [1] F. E. Cohen, J. W. Kelly, *Nature* **2003**, *426*, 905–909; J. W. Kelly, *N. Engl. J. Med.* **2005**, *352*, 722–723.
- [2] R. L. Hull, G. T. Westermark, P. Westermark, S. E. Kahn, *J. Clin. Endocrinol. Metab.* **2004**, *89*, 3629–3643.
- [3] A. E. Butler, J. Jang, T. Gurlo, M. D. Carty, W. C. Soeller, P. C. Butler, *Diabetes* **2004**, *53*, 1509–1516.
- [4] J. D. Knight, J. A. Hebda, A. D. Miranker, *Biochemistry* **2006**, *45*, 9496–9508.
- [5] F. Chiti, C. M. Dobson, *Annu. Rev. Biochem.* **2006**, *75*, 333–366.
- [6] J. D. Knight, A. D. Miranker, *J. Mol. Biol.* **2004**, *341*, 1175–1187.
- [7] S. A. Jayasinghe, R. Langen, *Biochemistry* **2005**, *44*, 12113–12119; J. A. Williamson, A. D. Miranker, *Protein Sci.* **2007**, *16*, 110–117; M. Apostolidou, S. A. Jayasinghe, R. Langen, *J. Biol. Chem.* **2008**, *283*, 17205–17210.
- [8] J. A. Hebda, A. D. Miranker, *Annu. Rev. Biophys.* **2009**, *38*, 125–152.
- [9] R. Tycko, *Curr. Opin. Struct. Biol.* **2004**, *14*, 96–103.
- [10] J. Janson, R. H. Ashley, D. Harrison, S. McIntyre, P. C. Butler, *Diabetes* **1999**, *48*, 491–498; B. Caughey, P. T. Lansbury, *Annu. Rev. Neurosci.* **2003**, *26*, 267–298. J. R. Brender, K. Hartman, K. R. Reid, R. T. Kennedy, A. Ramamoorthy, *Biochemistry* **2008**, *47*, 12680–12688.
- [11] R. Mishra, B. Bulic, D. Sellin, S. Jha, H. Waldmann, R. Winter, *Angew. Chem.* **2008**, *120*, 4757–4760; *Angew. Chem. Int. Ed.* **2008**, *47*, 4679–4682.
- [12] Y. Porat, Y. Mazor, S. Efrat, E. Gazit, *Biochemistry* **2004**, *43*, 14454–14462.
- [13] M. Levy, Y. Porat, E. Bacharach, D. E. Shaley, E. Gazit, *Biochemistry* **2008**, *47*, 5896–5904.
- [14] J. E. Gestwicki, G. R. Crabtree, I. A. Graef, *Science* **2004**, *306*, 865–869; J. F. Aitken, K. M. Loomes, B. Konarkowska, G. J. S. Cooper, *Biochem. J.* **2003**, *374*, 779–784.
- [15] Y. Porat, A. Abramowitz, E. Gazit, *Chem. Biol. Drug Des.* **2006**, *67*, 27–37; E. Gazit, *FASEB J.* **2002**, *16*, 77–83.
- [16] H. Yin, A. D. Hamilton, *Angew. Chem.* **2005**, *117*, 4200–4235; *Angew. Chem. Int. Ed.* **2005**, *44*, 4130–4163 and references therein; J. M. Davis, L. K. Tsou, A. D. Hamilton, *Chem. Soc. Rev.* **2007**, *36*, 326–334; J. Becerril, A. D. Hamilton, *Angew. Chem.* **2007**, *119*, 4555–4557; *Angew. Chem. Int. Ed.* **2007**, *46*, 4471–4473; J. M. Rodriguez, A. D. Hamilton, *Angew. Chem.* **2007**, *119*, 8768–8771; *Angew. Chem. Int. Ed.* **2007**, *46*, 8614–8617.
- [17] J. T. Ernst, J. Becerril, H. S. Park, H. Yin, A. D. Hamilton, *Angew. Chem.* **2003**, *115*, 553–557; *Angew. Chem. Int. Ed.* **2003**, *42*, 535–539; L. A. Estroff, C. D. Incarvito, A. D. Hamilton, *J. Am. Chem. Soc.* **2004**, *126*, 2–3.
- [18] I. Saraogi, C. D. Incarvito, A. D. Hamilton, *Angew. Chem.* **2008**, *120*, 9837–9840; *Angew. Chem. Int. Ed.* **2008**, *47*, 9691–9694.
- [19] L. A. Estroff, Ph. D. Dissertation, Yale University (New Haven), **2003**.
- [20] J. Plante, F. Campbell, B. Malkova, C. Kilner, S. L. Warriner, A. J. Wilson, *Org. Biomol. Chem.* **2008**, *6*, 138–146.
- [21] J. M. Ahn, S. Y. Han, *Tetrahedron Lett.* **2007**, *48*, 3543–3547.
- [22] J. Becerril, Ph. D. Dissertation, Yale University (New Haven), **2007**.
- [23] J. A. Hebda, I. Saraogi, M. Magzoub, A. D. Hamilton, A. D. Miranker, *Chem. Biol.* **2009**, *16*, 943–950.
- [24] X-ray structures: CCDC 725332 (*tert*-butyl ester of **1d**) contains the supplementary crystallographic data for this paper. These data can be obtained free of charge from The Cambridge Crystallographic Data Centre via www.ccdc.cam.ac.uk/data_request/cif.